Available online at www.sciencedirect.com
ScienceDirect
Scripta Materialia 59 (2008) 151–154
Scripta MATERIALIA
www.elsevier.com/locate/scriptamat

The strength of gold nanowire forests

R. Dou and B. Derby*

School of Materials, University of Manchester, Grosvenor Street, Manchester M1 7HS, UK

Received 18 January 2008; revised 12 February 2008; accepted 27 February 2008
Available online 8 March 2008

We have studied the compression yield strength of gold nanowire forests, with wire diameters in the range 30–80 nm, fabricated by electrodeposition into porous alumina templates. The yield strength as a function of wire diameter continues to follow the trend reported for larger Au columns, with the yield stress of 30 nm diameter columns exceeding 1.4 GPa. No significant work-hardening is observed at plastic strains up to 30%. Deformed nanowires show surface steps consistent with the nucleation of dislocations and their escape from the surface.
© 2008 Acta Materialia Inc. Published by Elsevier Ltd. All rights reserved.

Keywords: Plastic deformation; Nanowires; Nanoindentation

Uniaxial compression studies have shown that the yield strength of sub-micron gold columns increases dramatically with decreasing column diameter [1–3]. Possible explanations for this size effect in the deformation of small crystalline structures have been reviewed by Nix et al. and can be ascribed to two mechanisms [4]: (1) strain gradients, in which a gradient of plastic strain is accommodated by the generation of a geometrically stored population of dislocations, and (2) dislocation starvation, where the close proximity of a free surface and the associated image forces remove dislocations from the structure, requiring continuous nucleation of new dislocations to maintain deformation. The absence of strain gradients during uniaxial compression testing indicates that dislocation starvation is the most likely mechanism for the size effects seen in the deformation of sub-micron gold columns. To date the gold columns used in these compression tests have been fabricated by the focused ion beam (FIB) machining of bulk gold specimens and the smallest diameter columns achieved are reported at 180 nm [3]. Thus deformation experiments on gold structures with smaller dimensions require different fabrication methods. Wu et al. reported very high yield stresses obtained from gold wires in the size range 40–200 nm produced by electrolytic deposition using porous alumina templates [5]. However, these wires were tested in bending, which introduces significant strain gradients, possibly accounting for the extremely high yield stresses reported.

An alternative method to produce nanometer-scale gold structures is through the dealloying of Au_xAg_{1-x} solid solution alloys to produce nanoporous gold, which has an internal structure analogous to an open-cell foam with a sub-micron ligament diameter. A number of authors have reported the mechanical strength of nanoporous gold using a range of alloys of composition $0.25 < x < 0.42$ with ligament diameter ranging from 5 to 900 nm [6–10]. Yield strength data is obtained by deforming a large number of ligaments simultaneously, either through nanoindentation [6–10] or by the microfabrication of miniature components that are tested in compression [6] or in bend [9]. All these analyses of nanoporous gold have used an identical mechanical model to determine the behavior of the gold ligaments within the structure from the macroscopic mechanical properties of nanoporous gold. This model is that developed by Gibson and Ashby to analyse the mechanical properties of conventional open-cell foamed structures, where the length scale is typically in the range 10^{-4}–10^{-3} m [11,12]. The model represents the structure of an open-cell foam as a regular framework of square section ligaments; the dominant deformation mode of the members during macroscopic deformation of the foam is assumed to be bending of the ligaments and an accurate estimate of the elastic constants of the gold ligaments has been obtained [6–9]. The plastic deformation of the foam is modeled by the formation of plastic hinges at the ends of the ligaments. Within a plastic

* Corresponding author. E-mail: Brian.Derby@Manchester.ac.uk

1359-6462/$ - see front matter © 2008 Acta Materialia Inc. Published by Elsevier Ltd. All rights reserved.
doi:10.1016/j.scriptamat.2008.02.046

hinge there will be strain gradients that are unimportant in the relatively large scale foamed structures modeled by Gibson and Ashby but may be of greater significance in the deformation of nanoporous gold. Thus the yield stress reported in the literature from the deformation of nanoporous foams may reflect a combination of strain gradient and dislocation starvation strengthening mechanisms.

There is clearly a need to investigate the mechanical properties of gold wires and columns in the absence of strain gradients at diameters smaller than available by FIB machining. Here we report the uniaxial compressive mechanical properties of gold nanowires with diameters in the range 30–80 nm. This size range is comparable with the ligament diameter in many of the porous gold materials reported elsewhere.

We have fabricated gold nanowires by electrodeposition into the pores of a highly ordered anodic aluminum oxide (AAO) template with controlled pore diameter and spacing. We used the two-step anodization process pioneered by Masuda to make hexagonally ordered porous alumina membranes [13,14]. High-purity (99.999%) aluminum foils were degreased in acetone and electropolished in a mixture of perchloric acid and ethanol (1:4 by volume). The aluminum foil was anodized at a constant voltage of 40 V in 0.3 M oxalic acid solution at 10 °C for 12 h. The AAO film formed by this first anodization process was removed by etching in a chromic acid (0.1 M) and phosphoric acid (0.1 M) mixture at 60 °C for more than 1 h. To produce regular pores, a second anodizing step was then carried out under conditions identical to the first anodization for 2 h. This results in a hexagonal array of 30 nm diameter pores. In order to produce pores with different diameters, a phosphoric acid etch (0.1 M) was used at 30 °C; etching for 30 min and 60 min increased the mean pore diameter to approximately 55 nm and 80 nm, respectively.

To produce the required template for gold deposition, the surface of the AAO film was spin-coated with 2 g poly methyl methacrylate (PMMA) dissolved in 20 ml of acetone. Following this, the aluminum substrate was removed by etching in an aqueous copper chloride solution (0.1 M). The exposed alumina barrier layer at the base of the pores was eliminated by further etching with phosphoric acid (0.1 M) for 80 min at 30 °C. A gold layer was then sputtered onto the resulting ordered nanoporous AAO template to act as a new conductive substrate. The PMMA layer on the original AAO surface was removed by dissolution in acetone at 30 °C. Finally gold was electrodeposited into the pores of the AAO template using an electrolyte containing $KAu(CN)_2$ (0.02 M) and Na_2CO_3 (0.25 M) at pH 13. A three-electrode cell was used, with a sputter-coated AAO template working electrode, a platinum mesh counter electrode and an Ag/AgCl reference electrode operating at −1.2 V.

After deposition, the AAO template was partially etched away by 3 M NaOH solution in order to expose a forest of gold nanowires that are held vertical by the remaining AAO template. Scanning electron microscope (SEM) and transmission electron microscope (TEM) images of a representative gold nanowire forest are shown in Figure 1. The nanowires are straight and parallel with identical diameter, and height determined by the thickness of the anodized template. Individual gold nanowires are single crystals, each with a different crystal orientation. Electron backscatter diffraction analysis confirmed that the crystal orientation of each nanowire was random and that the nanowire forest showed no texture (Fig. 1c).

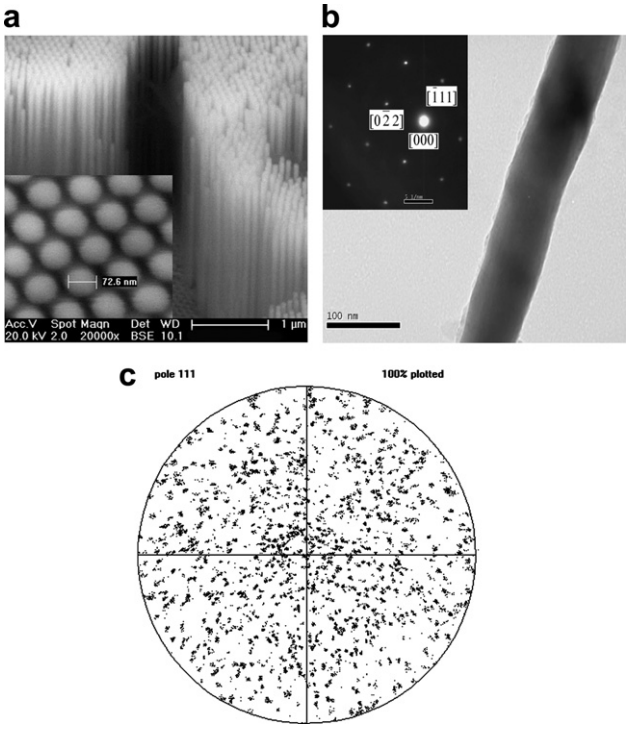

Figure 1. (a) SEM image of a free-standing gold nanowire forest, the inset shows a top view of the gold nanowires. (b) TEM image of a 80 nm diameter single crystal gold nanowire, the inset shows a (1 0 0) diffraction pattern. (c) The ⟨1 1 1⟩ pole figure obtained from a nanowire forest by electron backscatter diffraction showing a random texture.

Uniaxial compression tests on gold nanowire forests were conducted using a MTS Nanoindenter XP (MTS Nano Instruments, Oak Ridge, TN, USA), fitted with a 10 μm diameter cylindrical diamond flat punch tip. In each experiment the indenter was loaded at a constant loading rate (1 $\mu N\,s^{-1}$); when the prescribed maximum displacement was reached, the tip was held at peak load for 10 s and then unloaded. The load–displacement data obtained from the uniaxial compression tests were converted to stress and strain. The deformation of sub-micron gold columns is expected to be inhomogeneous [3], therefore engineering stress and strain can be used without loss of validity. Because the diameter of the flat punch tip is considerably greater than the diameter of the nanowires, a large number of individual nanowires are deformed in parallel and in simple compression during a single test. The mean diameter and number of deformed nanowires was determined from SEM images of the residual indent (Fig. 1). The average engineering stress in a single nanowire was thus determined with:

$$\bar{\sigma} = \frac{4F}{N\pi d^2} \tag{1}$$

where F is the load on the indenter, d is the mean diameter of the gold nanowires in the forest and N is the number of deformed nanowires. The number of nanowires in each indent was determined from individual SEM images and the apparent "missing" wires visible in Figure 2 accounted for.

Three nanowire forests with mean diameters 30, 60 and 70 nm were tested in compression and the resulting engineering stress–strain curves are plotted in Figure 3. The stress–strain data shows 3–5 superimposed measurements made at each wire diameter; no significant variation was seen within each set of measurements. The stress–strain curves show an initial linear increase in stress followed by a short non-linear response. This is followed by a plateau at constant stress. No significant increase in stress with plastic strain is seen. Finally, the trace shows the reduction in stress on unloading. The mean slope of the unloading curve is 79.4 GPa; this is very close to the Young's modulus of bulk gold, which is quoted as 80 GPa in a common reference text [15]. The elastic unloading indicates that no collapse of the high aspect ratio columns has occurred, presumably because of the stabilizing effect of the large column density and that no significant densification of the nanowire structure has occurred. The relative lack of features in these stress–strain data is believed to be the result of the measurements representing the average values obtained from many wires compressed in parallel ($N > 10^4$). In all cases the initial loading gradient is lower than the unloading response. This is probably because the flat punch is not coplanar with the top surface of the nanowire forest. No significant hardening of the wires was observed. The yield stress is taken as the plateau stress after 10% strain. The mean yield stress of the smallest gold nanowires, with 30 nm diameter, reaches 1.4 GPa. This value is much higher than the yield stress of bulk gold and is consistent with many of the reports on ligament yield in nanoporous gold [6–9]. The experimental results also show a strong size effect with the yield stress varying inversely with the diameter of the nanowires.

The yield stress data for the gold nanowire forests and previous results from the literature for the compression strength of gold nanocolumns and nanoporous gold are plotted in Figure 4. The yield strength of the porous gold, σ_p, has been replotted from the data in

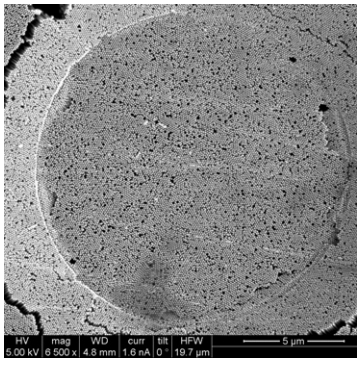

Figure 2. Residual indentation obtained after testing a section of the nanoforest in compression.

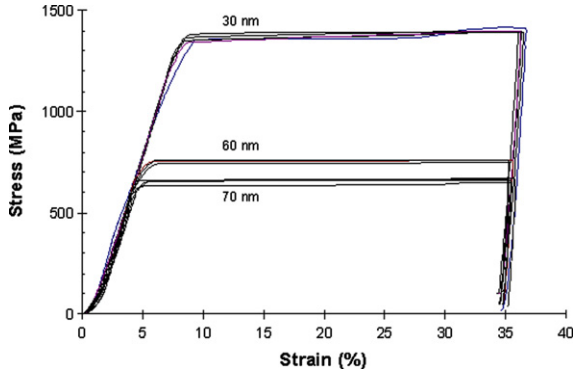

Figure 3. Engineering stress–strain curves from three gold nanoforests of mean diameter 30, 60 and 70 nm. There are 3–5 measurements plotted for each nanocolumn/nanowire diameter.

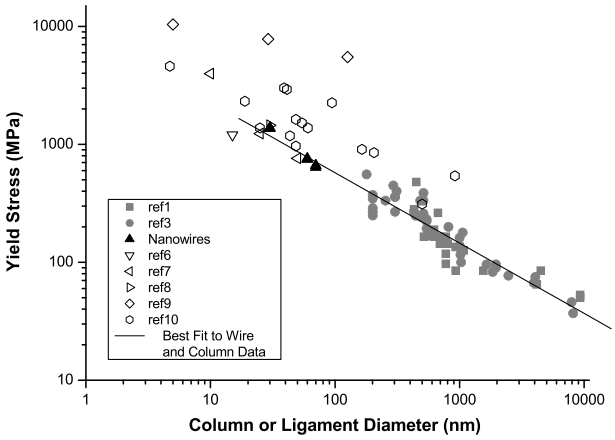

Figure 4. Yield stress as a function of diameter for the gold nanowires tested here in compression (black filled symbols), compression tests on larger gold nanocolumns produced by FIB milling (gray filled symbols) [1,3], and nanoporous gold specimens tested using a range of methods (open symbols) [6–10]. Line shows a linear fit to the combined nanowire and nanocolumn data.

Refs. [6–10]. The gold nanowire forest data lies on the same trend line obtained from the deformation of FIB machined gold columns with a dependence of yield stress, σ_Y, on column or wire diameter, d, given by the following empirical relation:

$$\sigma_Y = Kd^{-0.6} \tag{2}$$

where K is a constant. The yield stress obtained from the nanoporous gold specimens shows a greater scatter in yield stress for a given ligament diameter when comparing data obtained from different authors, although there is a general trend for smaller diameter ligaments yielding larger values of yield stress within each dataset. This may indicate subtle differences in the nanoporous microstructure obtained by different workers or possibly that the idealized geometry in the Gibson and Ashby model [11,12] does not capture the detailed plastic deformation of nanoporous gold.

TEM investigation was conducted to observe the effect of plastic deformation on the wires. The deformed nanowires were released into 3 M NaOH solution and dispersed on a carbon-coated TEM grid for observation.

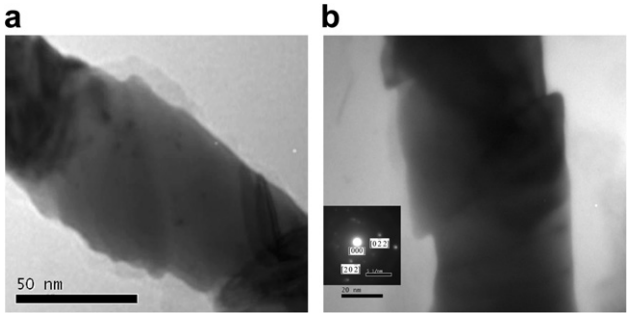

Figure 5. TEM images obtained from nanowires deformed by compression. (a) Step-like surface features and parallel shear indicates dislocation motion during deformation. (b) Surface steps; inset diffraction pattern indicates possible deformation twinning.

TEM images of nanowires after compression testing are given in Figure 5. The nanowires are released as individual wires after indentation with no interwire bonding. This supports the assumption that each wire has deformed independently and that the loading is similar to that which occurs in the deformation of isolated metal columns. The surfaces of the deformed nanowires show a stepped surface not evident in the undeformed wires. Similar surface steps have been found on the surfaces of larger diameter gold nanowire columns tested in compression [1–3]. The steps are believed to indicate the intersection of active dislocation slip planes with the nanowire surface. We were unable to identify the presence of dislocations in the deformed nanowires. These observations are consistent with the mechanism proposed by Nix et al. for hardening governed by dislocation starvation [1–4]. In this mechanism the presence of the free surface of a nanowire generates image stresses that attract dislocations to the surface, where they leave behind a slip step. This would account for the low density of dislocations in the deformed material and also explain the absence of work-hardening seen in the stress–strain response of the deforming nanoforests. The extensive slip stepping seen on all deformed nanowires confirms that dislocation slip is the dominant deformation mechanism. However, the diffraction pattern obtained from one deformed nanowire (Fig. 4b) shows a number of orientations. We did not see multiple grains in the undeformed nanowires and this may indicate the presence of deformation twinning. Twinning has been predicted in molecular dynamic studies of gold nanowire deformation [16] and has been found in other studies of the deformation of small volumes of gold [17].

In conclusion we have found that the yield strength of gold nanowires or nanocolumns, with diameters in the range 30–70 nm, follows the same size-dependent relation as has been reported for samples with diameter in the range 200–1000 nm. The maximum yield strength measured at approximately 1.4 GPa for 30 nm diameter nanowires is significantly higher than that expected from polycrystalline gold specimens. However, deformation appears to be by conventional mechanisms of dislocation motion and possibly twinning. Other workers have hypothesized that the strength of gold structures with dimensions similar to our nanowires approaches the ideal strength, although they quote a considerable range, 1.5–8 GPa, for the value of the ideal strength [18]. Despite this, we do not believe that our data from 30 nm nanowires showing a strength of 1.4 GPa, conclusively demonstrates that an upper limit to strength has been achieved and thus smaller structures may display still higher yield strength values if tested in compression.

[1] J.R. Greer, W.C. Oliver, W.D. Nix, Acta Mater. 53 (2005) 1821.
[2] J.R. Greer, W.D. Nix, Phys. Rev. B 73 (2006) 245410.
[3] C.A. Volkert, E.T. Lilleodden, Philos. Mag. 86 (2006) 5567.
[4] W.D. Nix, J.R. Greer, G. Feng, E.T. Lilleodden, Thin Solid Films 515 (2007) 3152.
[5] B. Wu, A. Heidelberg, J.J. Boland, Nature Mater. 4 (2005) 525.
[6] C.A. Volkert, E.T. Lilleodden, D. Kramer, J. Weissmuller, Appl. Phys. Lett. 89 (2006) 061920.
[7] J. Biener, A.M. Hodge, J.R. Hayes, C.A. Volkert, L.A. Zepeda-Ruiz, A.V. Hamza, F.F. Abraham, Nano Lett. 6 (2006) 2379–2382.
[8] D. Lee, X. Wei, X. Chen, M. Zhao, S.C. Jun, J. Hone, E.G. Herbert, W.C. Oliver, J.W. Kysara, Scripta Mater. 56 (2007) 437.
[9] M. Hakamada, M. Mabuchi, Scripta Mater. 56 (2007) 1003.
[10] A.M. Hodge, J. Biener, J.R. Hayes, P.M. Bythrow, C.A. Volkert, A.V. Hamza, Acta Mater. 55 (2007) 1343.
[11] L.J. Gibson, M.F. Ashby, Proc. R. Soc. Lond. A 382 (1982) 43.
[12] L.J. Gibson, M.F. Ashby, Cellular Solids: Structure and Properties, second ed., Cambridge University Press, Cambridge, 1997.
[13] H. Masuda, K. Fukuda, Science 268 (1995) 1466.
[14] H. Masuda, H. Yamada, M.H. Asoh, M. Nakao, T. Tamamura, Appl. Phys. Lett. 71 (1997) 2770.
[15] Metals Handbook, 10th ed., ASM International, Materials Park, OH, USA, 1990.
[16] H.S. Park, K. Gall, J.A. Zimmerman, J. Mech. Phys. Sol. 54 (2006) 1862.
[17] T. Kizuka, Phys. Rev. B 57 (1998) 11158.
[18] J. Biener, A.M. Hodge, A.V. Hamza, L.M. Hsiung, J.H. Satcher, J. Appl. Phys. 97 (2005) 024301.